Available online at www.sciencedirect.com
ScienceDirect
Dyes and Pigments 77 (2008) 31–38
www.elsevier.com/locate/dyepig

Effects of operational parameters on the decolorization of C.I. Reactive Red 198 in UV/TiO_2-based systems

Chung-Hsin Wu*

Department of Environmental Engineering, Da-Yeh University, 112, Shan-Jiau Road, Da-Tsuen, Chang-Hua 515, Taiwan, ROC

Received 31 January 2007; received in revised form 23 February 2007; accepted 2 March 2007
Available online 12 March 2007

Abstract

The effects of pH, dye concentration, electron acceptor (hydrogen peroxide, persulfate and copper ions) and hydroxyl radical trap (ethanol) on the decolorization of C.I. Reactive Red 198 using a UV/TiO_2 system were determined. Decolorization rate increased as the concentration of persulfate ions added increased. The *k* values followed the order: pH 4 > pH 7 > pH 10 for the UV/TiO_2, UV/TiO_2/H_2O_2 and UV/TiO_2/$Na_2S_2O_8$ systems. Hydrogen peroxide, persulfate and copper ions trapped photogenerated electrons and inhibited the recombination of electron/hole pairs in UV/TiO_2, thereby accelerating decolorization rate; persulfate ions trapped photogenerated electrons and generated sulfate free radicals. The addition of ethanol inhibited decolorization, suggesting that the predominant decolorization pathway involves hydroxyl radicals and that direct oxidation by photogenerated holes is also significant.

Keywords: UV; TiO_2; C.I. Reactive Red 198; Hydrogen peroxide; Persulfate; Copper; Ethanol

1. Introduction

Azo dyes, which contain one or more azo bonds, are the most widely used synthetic dyes and are major dye wastewater pollutants. Removing color from wastewater is more important than treating other colorless organics, because the presence of small amounts of dyes is clearly visible and detrimentally affects the water environment. In Taiwan, new strict regulations concerning discharged wastewater have been coupled with increased enforcement; accordingly, decolorization of dye effluents has attracted increased attention. Activated carbon and enhanced coagulation, which have been widely employed to remove refractory pollutants from textile wastewaters, are fairly effective in removing pollutants. However, these techniques transform dyes in solution into solid forms, such that the waste must be expensively post-treated. Advanced oxidation processes (AOPs) are alternative methods for decolorizing and reducing recalcitrant wastewater loads generated by textile companies. Most investigations of the photo-assisted decomposition of dyes have utilized TiO_2 as a model photocatalyst due to its chemical and biological stability, ready availability, cheapness, non-toxicity and high photocatalytic reactivity. Thus, TiO_2 was used in this work as photocatalyst.

AOPs generally involve the generation of the very powerful and non-selective oxidizing agent, hydroxyl radical ($OH^•$), to destroy hazardous pollutants. The following mechanism is the widely accepted to describe the photodegradation of organic compounds by UV/TiO_2 [1]. Photogenerated holes are generated as a result of TiO_2 particles having been irradiated with UV light (Eq. (1)). Hydroxyl radicals are produced by the oxidation of OH^- or H_2O by these photogenerated holes (Eqs. (2) and (3)) which are principally responsible for the destruction of organic species. Oxygen is used as an efficient electron trap (Eq. (4)), preventing the recombination of electrons and photogenerated holes. Eqs. (5)–(7) represent the other reactions of UV/TiO_2. If oxygen is limited, rapid recombination of photoproduced electrons and holes in TiO_2 lowers the efficiency of the photocatalytic reactions [2]; consequently,

---

* Fax: +886 5 5334958.
E-mail address: chunghsinwu@yahoo.com.tw

0143-7208/$ - see front matter © 2007 Elsevier Ltd. All rights reserved.
doi:10.1016/j.dyepig.2007.03.003

the usefulness of such a system has limited practical application.

$$TiO_2 + h\nu \rightarrow TiO_2(e_{CB-} + h_{VB+}) \quad (1)$$

$$TiO_2(h_{VB+}) + OH^- \rightarrow TiO_2 + OH^{\bullet} \quad (2)$$

$$TiO_2(h_{VB+}) + H_2O \rightarrow TiO_2 + H^+ + OH^{\bullet} \quad (3)$$

$$TiO_2(e_{CB-}) + O_2 \rightarrow TiO_2 + O_2^{-}\bullet \quad (4)$$

$$O_2^{-}\bullet + H^+ \rightarrow HO_2^{\bullet} \quad (5)$$

$$TiO_2(e^{\bullet}_{CB-}) + H^+ + O_2^{-}\bullet \rightarrow TiO_2 + HO_2^{-} \quad (6)$$

$$HO_2^{-} + H^+ \rightarrow H_2O_2 \quad (7)$$

Serpone et al. [2] proposed an interparticle electron transfer process (IPET) in which two semiconductors of different redox energy levels are combined so that the charge separation of the corresponding conduction and valance bands are increased, thereby enhancing the photocatalytic reaction efficiency of the two semiconductors [2–5]. However, the combined IPET photocatalysts must be carefully selected according to their redox energy levels and not all coupled photocatalysts effectively retard the recombination of photogenerated electrons and holes. Numerous studies have proposed that the addition of oxidants, such as H_2O_2 [1,6–17], $S_2O_8^{2-}$ [1,6,7,10–18], HSO_5^- [6] and BrO_3^- [11,13,16,17], eliminates the recombination process as the added oxidants rapidly react with conduction band electrons, generating extremely reactive oxidizing radicals, which increases the efficiency of TiO_2. Consequently, an electron acceptor (H_2O_2 and $Na_2S_2O_8$) was used in this investigation to inhibit the recombination of electron/hole pairs and improve the photodegradation efficiency of UV/TiO_2.

Liang et al. [19] demonstrated that transition metal ions can activate sodium persulfate to generate the sulfate free radical ($SO_4^-\bullet$), which is a powerful oxidant (of redox potential 2.6 V) and which can potentially degrade organics; in this context, Cu^{2+} ions were incorporated into UV/TiO_2/oxidant systems.

C.I. Reactive Red 198 (RR198) was selected for use in this work as the dye has two of the most commonly used anchor groups employed in reactive dyes, namely the monochlorotriazine and vinyl sulfone groups. The objectives of this investigation were to:

- determine the effects of dye concentration on decolorization efficiency;
- elucidate the impact of $Na_2S_2O_8$ dosage on decolorization efficiency;
- evaluate the effect of pH on various UV/TiO_2-based systems;
- determine the effects of adding hydrogen peroxide, persulfate ions, copper ions and ethanol on the UV/TiO_2 system;
- measure the effects of Cu^{2+} on both UV/TiO_2/$Na_2S_2O_8$ and UV/TiO_2/H_2O_2 systems.

2. Materials and methods

2.1. Materials

The TiO_2 catalyst was *Degussa P-25* (specific surface area, 50 m^2/g). C.I. reactive Red 198 (formula, M_r and λ_{max} were $C_{27}H_{18}ClN_7Na_4O_{15}S_5$, 967.5 g/mol and 520 nm, respectively) was obtained from Aldrich. Fig. 1(a) and 1(b) shows the chemical structure and UV–vis spectra of RR198, respectively. The λ_{max} of RR198 did not vary with pH (Fig. 1(b)). Copper nitrate ($Cu(NO_3)_2$), sodium persulfate ($Na_2S_2O_8$), hydrogen peroxide solution (H_2O_2, 30% w/w) and ethanol (C_2H_5OH) were obtained from Merck. pH was controlled using $HClO_4$ and NaOH via an automatic titrator. All reagents were of analytical grade and used without further treatment. Water was deionized and doubly distilled with Milli-Q.

2.2. Decolorization experiments

The dye concentration was 20 ppm in all experiments, except in the case of experiments designed to determine the effect of dye concentrations on the UV/TiO_2 system. Decolorization experiments were conducted in a 3-L, hollow cylindrical glass reactor, using a 500 W medium-pressure, 300 mW cm^{-2} Hg lamp (254 nm, Philips) placed inside a quartz tube as irradiation source. In all UV/TiO_2-based systems used, the TiO_2 dosage was 0.5 g L^{-1}. The concentrations of copper ions and hydrogen peroxide were 0.5 and 0.33 mM, respectively; persulfate ion doses of 0.1, 0.2, 0.5, 1 and 2 mM were used to determine the effect of persulfate ion dosage. All systems were stirred at 300 rpm and aerated continuously. Aliquots (15 mL) were withdrawn from the photoreactor at pre-specified intervals;

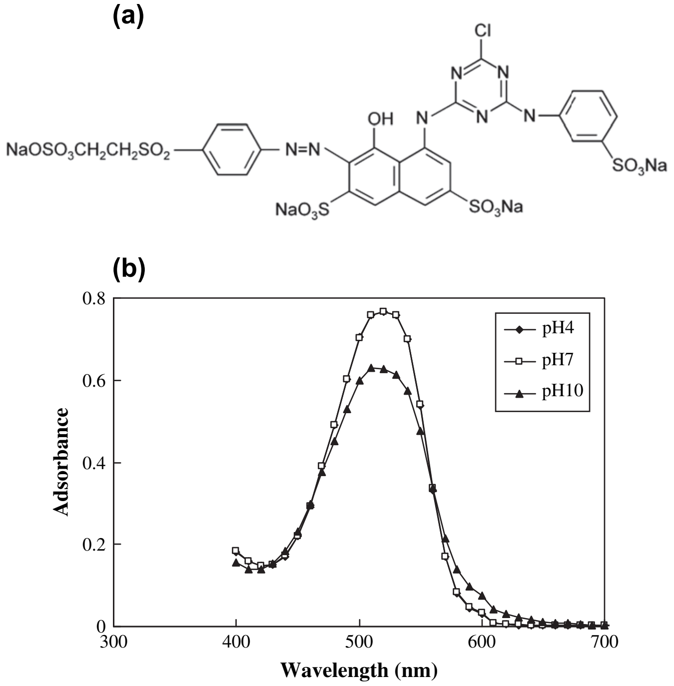

Fig. 1. Characteristics of RR198 (a) chemical structure and (b) UV–vis spectra.

suspended TiO_2 particles were separated by centrifuging at 5000 rpm for 10 min followed by filtration through a 0.22 μm filter (Millipore). The dye concentration was measured using a spectrophotometer (Hitachi U-2001) at 520 nm; decolorization efficiency was determined from the difference between dye concentrations before and after each experiment. Ionic chromatography (Dionex DX-120) was utilized to determine the concentrations of sulfate, nitrate and chloride anions. The extent of mineralization of RR198 was identified by the reduction in total organic carbon (TOC), as determined using an O.I. 1010 TOC analyzer.

3. Results and discussion

3.1. Effects of dye and persulfate ion concentration

Adsorption of TiO_2, direct degradation by H_2O_2 or $Na_2S_2O_8$, and dye photolysis were evaluated at pH 7 (Fig. 2). Adsorption and direct degradation revealed no significant disappearance of RR198; as the decolorization rate of RR198 was extremely low ($0.0117\ min^{-1}$), subsequent decolorization in UV/TiO_2-based systems could be attributed to photocatalytic reaction.

3.1.1. Effect of dye concentration

The effect of initial dye concentration on the rate of dye decolorization was determined by varying the initial dye concentration at 10, 20, 40, 60 and 80 ppm at pH 7 in the UV/TiO_2 system (Fig. 3(a)). Plotting $\ln(C_0/C)$ as a function of time yielded the decolorization rate constant (k) (Fig. 3(b)), values of which were consistent with pseudo-first-order kinetics as found by other workers [1,4,18,20,21]. As the decolorization efficiency can be described in terms of k value, Table 1 shows that the k values for 10, 20, 40, 60 and 80 ppm RR198 for the UV/TiO_2 system were 0.2424, 0.1018, 0.0433, 0.0333 and $0.0226\ min^{-1}$, respectively; clearly, the decolorization rate constant declined as dye concentration increased. Several studies have obtained similar experimental findings for UV/TiO_2-based systems [1,8,12,16,17,21,22]. This phenomenon has three possible explanations.

(i) A significant quantity of UV light may be absorbed by the highly concentrated dye molecules rather than by the TiO_2 particles, thereby reducing decolorization efficiency; the dye therefore has a UV-screening effect insofar as, fewer photons reach the TiO_2 surface as dye

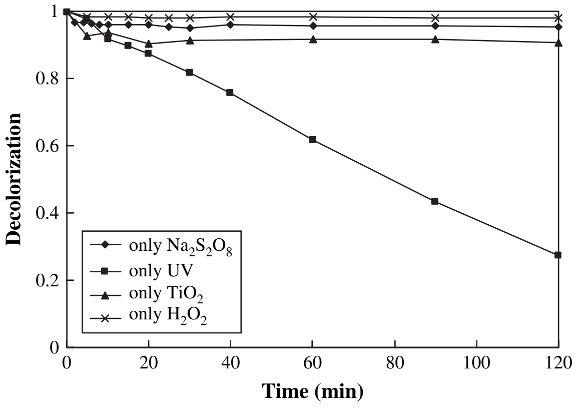

Fig. 2. Adsorption, direct degradation and photolysis of RR198 at pH 7 (RR198 = 20 ppm, TiO_2 = 0.5 g/L, $Na_2S_2O_8$ = 0.5 mM, H_2O_2 = 0.33 mM and 25 °C).

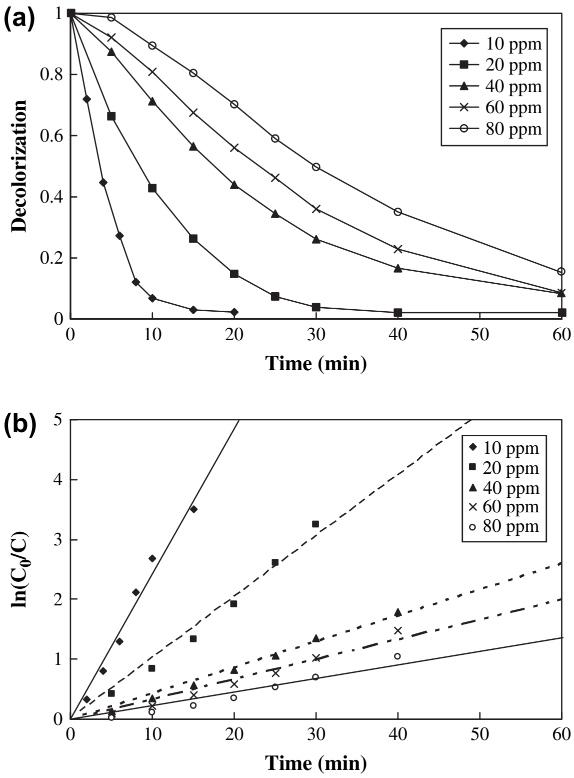

Fig. 3. Effects of dye concentration in UV/TiO_2 system at pH 7: (a) decolorization efficiency and (b) linear regression of pseudo-first-order reaction kinetics (TiO_2 = 0.5 g/L and T = 25 °C).

Table 1
Effects of initial concentration of dye and $Na_2S_2O_8$ on decolorization rate constants (k, min^{-1}) (TiO_2 = 0.5 g/L, pH = 7 and 25 °C)

Effects of dye concentration in UV/TiO_2

Dye conc. (ppm)	k (min^{-1})	R^2
10	0.2424	0.9731
20	0.1018	0.9840
40	0.0433	0.9854
60	0.0333	0.9539
80	0.0226	0.9109

Effects of $Na_2S_2O_8$ concentration in UV/TiO_2 (dye = 20 ppm)

$Na_2S_2O_8$ conc. (mM)	k (min^{-1})	R^2
0.1	0.1415	0.9974
0.2	0.1432	0.9985
0.5	0.1683	0.9958
1	0.1837	0.9764
2	0.2109	0.9868

concentration increase, slowing the formation of hydroxyl radicals.

(ii) As the initial concentration of dye increased, the TiO_2 surfaces adsorbed additional dye molecules which inhibited direct contact between the dye molecules and photogenerated holes [8] and which also suppressed the generation of hydroxyl radicals at the TiO_2 surface as dye molecules covered active surface sites [1].

(iii) Increased amounts of dye and reaction intermediates competed with both hydroxyl radicals and active reaction sites at the TiO_2 surface, as the initial dye concentration increased. Since the amount of TiO_2 remained constant, the rate of formation of hydroxyl radicals at the TiO_2 surface was constant. Hence, the fraction of hydroxyl radicals that attacks the dye molecules and its reaction intermediates declined as the dye concentration increased.

3.1.2. Effects of concentration of persulfate ions

Fig. 4 shows the effects of persulfate ion dosage on decolorization efficiency. The k values obtained when 0, 0.1, 0.2, 0.5, 1 and 2 mM persulfate ions were added were 0.1018, 0.1415, 0.1432, 0.1683, 0.1837 and 0.2109 min^{-1}, respectively (Table 1). Thus, the decolorization rate increased as the dosage of persulfate ions increased. Persulfate ions trap photogenerated electrons, preventing their recombination with positive holes, while simultaneously producing sulfate free radicals (Eq. (8)) [1,14] which can react with water molecules to generate hydroxyl radicals (Eq. (9)) [1]. Dogliotti and Hayon [23] and Ivanov et al. [24] showed that persulfate ions undergo photolysis under light irradiation, forming sulfate free radicals (Eq. (10)). According to Eqs. (8)–(10), increased amounts of persulfate ions generated additional sulfate free radicals and hydroxyl radicals which accelerated decolorization. Various studies have demonstrated that reactive radical intermediates, generated from persulfate ions reacting with photogenerated electrons, accelerate decolorization in the $UV/TiO_2/S_2O_8^{2-}$ system [1,6,7,11–15,17,18].

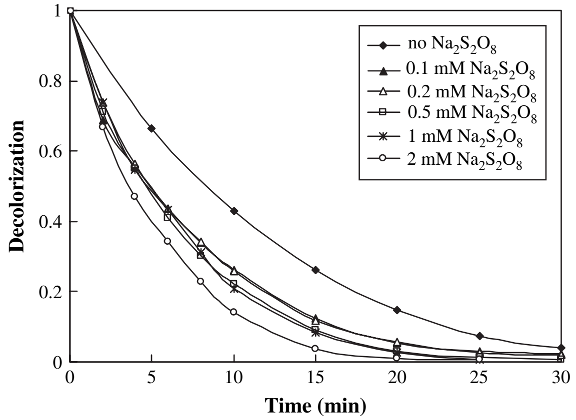

Fig. 4. Effects of $Na_2S_2O_8$ dose in $UV/TiO_2/Na_2S_2O_8$ system ($RR198 = 20$ ppm, $TiO_2 = 0.5$ g/L, pH = 7 and $T = 25$ °C).

$$S_2O_8^{2-} + e_{CB-} \rightarrow SO_4^{2-} + SO_4^{-}\bullet \tag{8}$$

$$SO_4^{-}\bullet + H_2O \rightarrow SO_4^{2-} + H^+ + OH^{\bullet} \tag{9}$$

$$S_2O_8^{2-} + h\nu \rightarrow 2SO_4^{-}\bullet \tag{10}$$

3.2. Effect of pH on decolorization efficiency

The decolorization efficiency of the UV/TiO_2, $UV/TiO_2/Na_2S_2O_8$ and $UV/TiO_2/H_2O_2$ systems was determined at pH 4, 7 and 10 (Fig. 5). After 10 min of reaction, the decolorization of UV/TiO_2 at pH 4, 7 and 10 was 98%, 57% and 35%, respectively, that of $UV/TiO_2/Na_2S_2O_8$ was 99%, 78% and 48%, respectively and that of $UV/TiO_2/H_2O_2$ was 99%, 84% and 51%, respectively. The k values for the UV/TiO_2, $UV/TiO_2/Na_2S_2O_8$ and $UV/TiO_2/H_2O_2$ systems increased as pH decreased (Table 2).

As pH influences the surface properties of TiO_2, dissociation of dye and formation of hydroxyl radicals, interpreting the effects of pH on degradation efficiency is extremely difficult. Notably, pH influences the adsorption of dye molecules on the TiO_2 surface, which is an important step in photodegradation. As the isoelectric point (pH_{IEP}, which is that pH at which the zeta potential is zero) of TiO_2 is 6.6 [25], the surface of TiO_2 will be positively charged at $pH < pH_{IEP}$. As the dye is anionic and negatively charged due to the sulfonate groups, electrostatic interaction between the TiO_2 surface and dye anions resulted in adsorption at $pH < 6.6$, which would explain the observed high decolorization rate. Conversely, dye adsorption onto the TiO_2 surfaces will be low at $pH > 6.6$ because of electrostatic repulsion between the negatively charged TiO_2 surfaces and the anionic dye molecules. Thus, the k values followed the order: pH 4 > pH 7 > pH 10 in UV/TiO_2, $UV/TiO_2/Na_2S_2O_8$ and $UV/TiO_2/H_2O_2$ systems (Table 2). Since numerous reaction mechanisms are involved in dye degradation, including hydroxyl radical attack, direct oxidation by positive holes and direct reduction by electrons, the effect of pH on degradation efficiency differs from that of photocatalysts and model substrates.

The k values of the $UV/TiO_2/Na_2S_2O_8$ system at pH 4, 7 and 10 were 0.6077, 0.1683 and 0.0683 min^{-1}, respectively (Table 2). Fig. 4 presents the synergistic effect of the persulfate on the UV/TiO_2 system. The acceleration of the decolorization process depends on solution pH; under acidic conditions, persulfate ions are acid-catalyzed as persulfate free radicals (Eqs. (11) and (12)) [26] whereas in alkaline solution, as persulfate free radicals are converted to hydroxyl radicals (Eq. (13)) [23]. It is therefore proposed that persulfate free radicals are the dominant oxidant under acidic conditions whereas the hydroxyl radical is the dominant oxidant under alkaline conditions.

$$S_2O_8^{2-} + H^+ \rightarrow HS_2O_8^{-} \tag{11}$$

$$HS_2O_8^{-} \rightarrow SO_4^{2-} + H^+ + SO_4^{-}\bullet \tag{12}$$

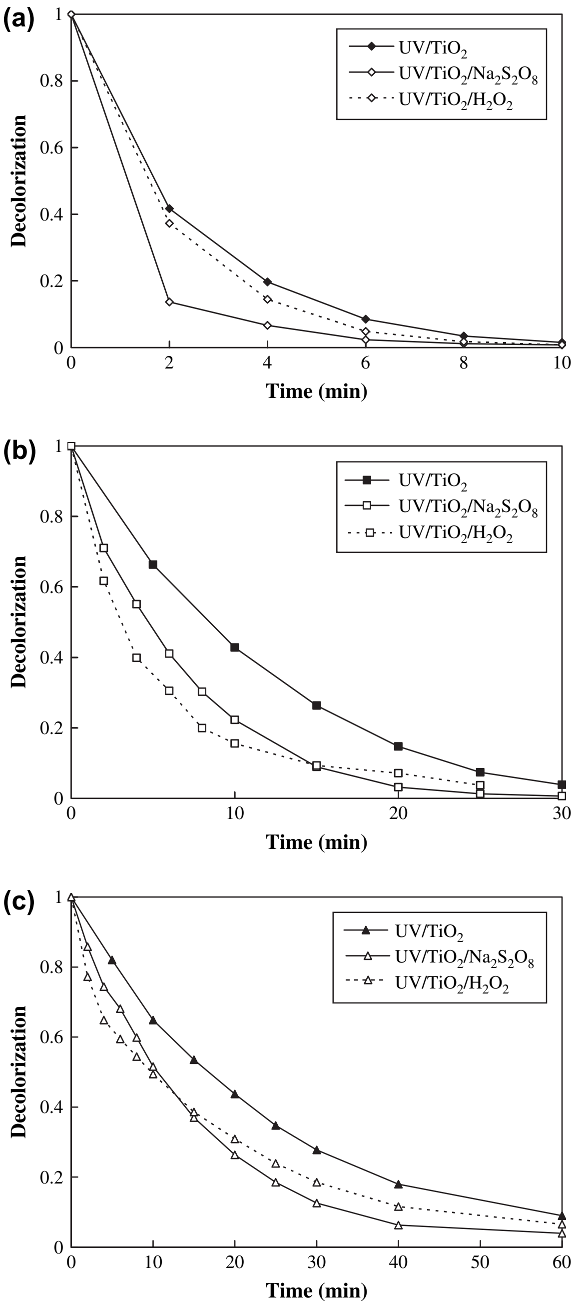

Fig. 5. Decolorization efficiency of UV/TiO$_2$, UV/TiO$_2$/Na$_2$S$_2$O$_8$ and UV/TiO$_2$/H$_2$O$_2$ systems at various pHs: (a) pH 4, (b) pH 7 and (c) pH 10 (RR198 = 20 ppm, TiO$_2$ = 0.5 g/L, Na$_2$S$_2$O$_8$ = 0.5 mM, H$_2$O$_2$ = 0.33 mM and 25 °C).

$$SO_4^{-}\bullet + H_2O \rightarrow SO_4^{2-} + OH^{\bullet} + H^{+} \quad (13)$$

Although H$_2$O$_2$ did not decolorize RR198 (Fig. 2), combining H$_2$O$_2$ with UV/TiO$_2$ markedly improved the decolorization efficiency; the k values for the UV/TiO$_2$/H$_2$O$_2$ system at pH 4, 7 and 10 were 0.5020, 0.1771 and 0.0517 min^{-1}, respectively (Table 2). Eqs. (14)–(16) describe how the addition of H$_2$O$_2$ to the UV/TiO$_2$ system promoted decolorization. Firstly, H$_2$O$_2$ photolysis yielded hydroxyl radicals via UV irradiation (Eq. (14)) and then H$_2$O$_2$ trapped photogenerated electrons (Eq. (15)) and inhibited the recombination of the photogenerated electron/hole pairs; finally, H$_2$O$_2$ reacted with the UV/TiO$_2$ intermediate ($O_2^{-\bullet}$) (Eq. (16)) and generated hydroxyl radicals. Accordingly, adding H$_2$O$_2$ accelerated the decolorization rate of the UV/TiO$_2$ system; several studies have reported similar results [1,6–17].

$$H_2O_2 + h\nu \rightarrow 2OH^{\bullet} \quad (14)$$

$$H_2O_2 + e_{CB-} \rightarrow OH^{-} + OH^{\bullet} \quad (15)$$

$$H_2O_2 + O_2^{-}\bullet \rightarrow OH^{-} + OH^{\bullet} + O_2 \quad (16)$$

The degradation rate of organic compounds typically increases with H$_2$O$_2$ dosage up to a critical value; as the H$_2$O$_2$ dose increases further, degradation efficiency declines since H$_2$O$_2$ scavenges hydroxyl radicals when present at high concentrations [27,28], yielding hydroperoxyl radicals that have lower oxidation capacity than hydroxyl radicals (Eq. (17)). Furthermore, recombination of hydroxyl radicals reduces decolorization efficiency (Eq. (18)). Hence, the amount of H$_2$O$_2$ in the UV/TiO$_2$/H$_2$O$_2$ system must be controlled carefully.

$$OH^{\bullet} + H_2O_2 \rightarrow HO_2^{\bullet} + H_2O \quad (17)$$

$$2OH^{\bullet} \rightarrow H_2O_2 \quad (18)$$

pH influences the production of hydroxyl radicals and, therefore, decolorization efficiency. The k values for the UV/TiO$_2$/H$_2$O$_2$ system followed the order: pH 4 > pH 7 > pH 10, perhaps resulting from the auto-decomposition of H$_2$O$_2$ to oxygen and water under alkaline conditions and the influence of dye–TiO$_2$ adsorption. As Buxton et al. [29] proposed that the oxidation potential of hydroxyl radicals decreases with increasing pH, the decolorization rate constant was lowest at pH 10 in all UV/TiO$_2$/oxidant systems.

3.3. Comparisons of UV/TiO$_2$-based systems

Figs. 6 and 7 compare the decolorization efficiencies achieved for the UV/TiO$_2$-based systems at pH 4 and 7, respectively. This investigation evaluated the effects of adding copper ions to the UV/TiO$_2$/oxidant systems at pH 4 (Fig. 6) and adding ethanol to the UV/TiO$_2$ systems at pH 7 (Fig. 7). The observed synergistic effect was typically greater when persulfate ions had been added to the UV/TiO$_2$ system than when hydrogen peroxide was used (Table 2). The one-electron reduction potentials of the species of interest are $E(O_2/O_2^{-\bullet}) = -155$ mV, $E(H_2O_2/OH^{\bullet}) = 800$ mV and $E(S_2O_8^{2-}/SO_4^{-\bullet}) = 1100$ mV [30]. Thermodynamically, H$_2$O$_2$ and $S_2O_8^{2-}$ are more efficient electron acceptors than molecular oxygen and $S_2O_8^{2-}$ is more efficient than H$_2$O$_2$. Numerous studies have shown that $S_2O_8^{2-}$ is a stronger electron acceptor than H$_2$O$_2$ [6,7,12,14,17]. However, Qamar et al. [11] and Tariq et al. [13] obtained the opposite result, which indicated that H$_2$O$_2$ was a stronger electron trap than $S_2O_8^{2-}$ in the UV/TiO$_2$ system for *Chromotrope 2B* and *Amaranth*. The discrepancies between their studies and this investigation may be attributed to differences between pH values and parent compounds in the UV/TiO$_2$/oxidant systems.

Table 2
Decolorization rate constants (k, min^{-1}) and correlation coefficients of UV/TiO_2-based systems

	pH 4		pH 7		pH 10	
	k	R^2	k	R^2	k	R^2
UV/TiO_2	0.4165	0.9996	0.1018	0.9840	0.0414	0.9975
UV/TiO_2/$Na_2S_2O_8$	0.6077 (1.0903)[a]	0.9274 (0.9444)[a]	0.1683	0.9958	0.0683	0.9991
UV/TiO_2/H_2O_2	0.5020 (0.5662)[b]	0.9993 (0.9074)[b]	0.1771	0.9489	0.0517	0.9410

RR198 = 20 ppm, TiO_2 = 0.5 g/L, $Na_2S_2O_8$ = 0.5 mM, H_2O_2 = 0.33 mM, Cu^{2+} = 0.5 mM and 25 °C.

[a] The values denoted the results of UV/TiO_2/$Na_2S_2O_8$/Cu system.

[b] The values showed the results of UV/TiO_2/H_2O_2/Cu system.

Interestingly, the addition of copper ions to the UV/TiO_2/$Na_2S_2O_8$ and UV/TiO_2/H_2O_2 systems increased the decolorization rate (Fig. 6); the k values for UV/TiO_2/$Na_2S_2O_8$, UV/TiO_2/H_2O_2, UV/TiO_2/$Na_2S_2O_8$/Cu and UV/TiO_2/H_2O_2/Cu systems at pH 4 were 0.6077, 0.5020, 1.0903 and 0.5662 min^{-1}, respectively (Table 2). The observed increase in decolorization rate can be attributed to electron trapping at the TiO_2 surface, which prevents electron–hole recombination and, thereby, accelerates the formation of hydroxyl radicals. In the UV/TiO_2/$Na_2S_2O_8$/Cu system, Cu^{2+} trapped the photogenerated electrons and was reduced to Cu^+ (Eq. (19)) which reacted with persulfate ions to generate persulfate free radicals (Eqs. (20)–(22)) [26]; moreover, Cu^{2+} reacts directly with persulfate ions to produce persulfate free radicals (Eq. (23)) [26]. Based on Eqs. (19)–(23), adding Cu^{2+} inhibits recombination of photogenerated electron/hole pairs and produces additional persulfate free radicals in the UV/TiO_2/$Na_2S_2O_8$ system, thereby accelerating decolorization.

$$Cu^{2+} + e_{CB-} \rightarrow Cu^{+} \tag{19}$$

$$Cu^{+} + S_2O_8^{2-} \rightarrow CuS_2O_8^{-} \tag{20}$$

$$CuS_2O_8^{-} \rightarrow Cu^{2+} + SO_4^{2-} + SO_4^{-}\bullet \tag{21}$$

$$SO_4^{-}\bullet + Cu^{+} \rightarrow Cu^{2+} + SO_4^{2-} \tag{22}$$

$$Cu^{2+} + S_2O_8^{2-} \rightarrow Cu^{3+} + SO_4^{2-} + SO_4^{-}\bullet \tag{23}$$

Skoumal et al. [31] suggested that additional hydroxyl radicals can be produced by the Cu^{2+}/Cu^{+} pair, since Cu^{2+} can be reduced with the $HO_2^{\bullet}$ formed from Eq. (5) to give Cu^{+} (Eq. (24)), which can be further oxidized by the H_2O_2 generated through Eq. (7) to Cu^{2+} and hydroxyl radicals (Eq. (25)). In the UV/TiO_2/H_2O_2/Cu system, Eqs. (19) and (25) formed cyclic reactions as an additional source of hydroxyl radical formation, resembling Fenton-like reactions [32]. The beneficial effect of copper ions is also attributable to the formation of a complex between the pollutant and copper ions that brings the copper ions close to the catalyst surface, enabling copper ions and TiO_2 to participate in the photoredox cyclic reaction, which yields oxidant species [33].

$$Cu^{2+} + HO_2^{\bullet} \rightarrow Cu^{+} + H^{+} + O_2 \tag{24}$$

$$Cu^{+} + H_2O_2 \rightarrow Cu^{2+} + HO^{\bullet} + OH^{-} \tag{25}$$

Adding ethanol reduced the decolorization rate of the UV/TiO_2 system (Fig. 7), the k value of UV/TiO_2 for the addition of 1% and 5% ethanol were 0.0322 and 0.0318 min^{-1}, respectively. Previous studies have demonstrated that ethanol quenches hydroxyl radicals, thereby reducing photodegradation rate [8,9]. This work found that small amounts of ethanol suppressed RR198 decolorization, implying that hydroxyl radicals are involved in decolorization. However, decolorization was not entirely prevented by the addition of 5% ethanol, which suggests that another reactive species, which does not react with ethanol, is involved in decolorization. This species

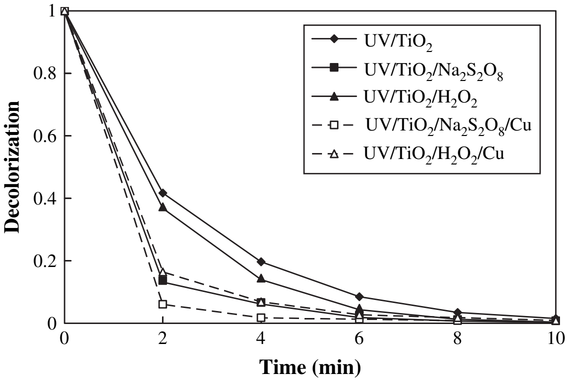

Fig. 6. Comparison of decolorization efficiency in UV/TiO_2-based systems at pH 4 (RR198 = 20 ppm, TiO_2 = 0.5 g/L, $Na_2S_2O_8$ = 0.5 mM, H_2O_2 = 0.33 mM, Cu^{2+} = 0.5 mM and 25 °C).

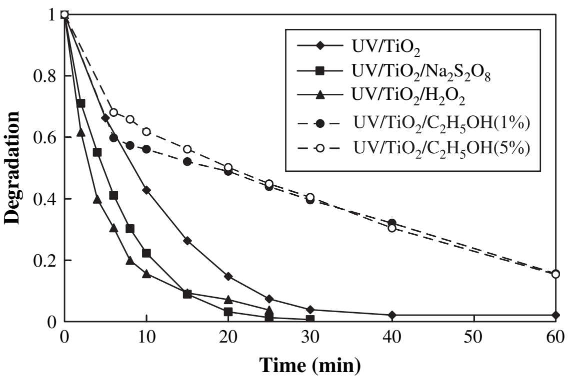

Fig. 7. Comparison of decolorization efficiency in UV/TiO_2-based systems at pH 7 (RR198 = 20 ppm, TiO_2 = 0.5 g/L, $Na_2S_2O_8$ = 0.5 mM, H_2O_2 = 0.33 mM, C_2H_5OH = 1% or 5% and 25 °C).

is most likely to be the photogenerated holes that are produced by the irradiated TiO_2. The inhibiting effect achieved of ethanol indicates that the primary decolorization pathway involves hydroxyl radicals and that direct oxidation by photogenerated holes is likely not negligible; numerous studies have obtained similar results [8,9].

Fig. 8 shows the dissociated concentration of sulfate during decolorization in the UV/TiO_2, UV/TiO_2/$Na_2S_2O_8$ and UV/TiO_2/H_2O_2 systems at pH 4; Table 3 presents the concentrations of Cl^-, NO_3^-, SO_4^{2-} and TOC in various UV/TiO_2-based systems after 30 min. The theoretical dissociation concentrations of Cl^-, NO_3^-, SO_4^{2-} and TOC for 20 ppm RR198 were 0.73, 8.97, 9.92 and 6.70 ppm, respectively; the theoretical SO_4^{2-} generated concentration of 0.5 mM $Na_2S_2O_8$ was 96 ppm. The concentration of dissociated sulfate in the UV/TiO_2/$Na_2S_2O_8$ system significantly exceeded that in the UV/TiO_2 and UV/TiO_2/H_2O_2 systems (Fig. 8 and Table 3) because persulfate ions decomposed to sulfate ions. Despite the fact that the dye was completely decolorized after 30 min in the UV/TiO_2, UV/TiO_2/$Na_2S_2O_8$ and UV/TiO_2/H_2O_2 systems at pH 4 (Fig. 5(a)), the dissociated concentrations of Cl^-, NO_3^-, SO_4^{2-} and TOC in various UV/TiO_2-based systems were lower than their respective theoretical values. Mahmoodi et al. [21], showed that the dissociated concentrations of Cl^-, NO_3^- and SO_4^{2-} of 50 ppm RR198 in a UV/TiO_2/H_2O_2 system after an irradiation period of 240 min were 2.5, 0.18 and 9.5 ppm, respectively, and obtained experimental results that were also lower than the theoretical values. This finding might be explained by the following two factors:

(i) dissociated Cl^-, NO_3^- and SO_4^{2-} were adsorbed onto the positively charged TiO_2 surfaces (at pH 4);
(ii) Cl, N and S atoms were incorporated into intermediates.

After reaction for 30 min, the TOC degradation efficiency was only 43–46% in the UV/TiO_2-based systems, even though the RR198 had been completely decolorized. Before treatment, the UV–vis spectra of RR198 consisted of three main absorption bands, two in the UV region (287 and 370 nm) [34] and one in the visible region (520 nm) (Fig. 1(b)). The UV band can be assigned to aromatic (benzene and naphthalene) rings present in azo dye molecules [35]. After reaction for 130 min in UV/TiO_2/H_2O_2, all absorbance peaks disappeared and no absorbance peaks existed in the UV–vis spectrum [21]. Mahmoodi et al. [21] determined that the primary intermediates of RR198 in the UV/TiO_2/H_2O_2 system were formate and oxalate anions, which were further oxidized slowly to CO_2.

Table 3
Analyses of IC and TOC in various UV/TiO_2-based systems

Unit (ppm)	UV/TiO_2	UV/TiO_2/$Na_2S_2O_8$	UV/TiO_2/H_2O_2
Cl^-	0.09	0.19	0.10
NO_3^-	<0.01	0.50	0.25
SO_4^{2-}	3.41	83.65	5.23
TOC	3.60	3.60	3.82

RR198 = 20 ppm, TiO_2 = 0.5 g/L, $Na_2S_2O_8$ = 0.5 mM, H_2O_2 = 0.33 mM, reaction time = 30 min, pH 4 and 25 °C.

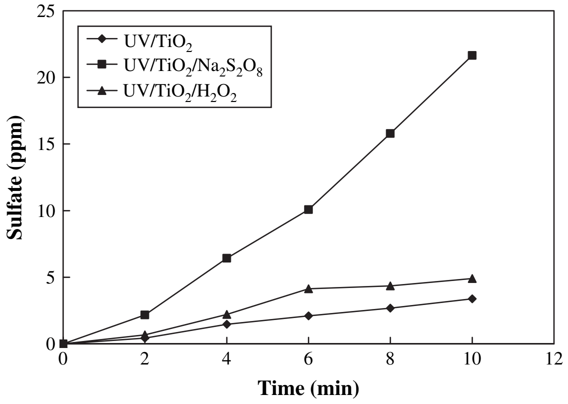

Fig. 8. Dissociated concentration of sulfate during decolorization in UV/TiO_2, UV/TiO_2/$Na_2S_2O_8$ and UV/TiO_2/H_2O_2 systems (RR198 = 20 ppm, TiO_2 = 0.5 g/L, $Na_2S_2O_8$ = 0.5 mM, H_2O_2 = 0.33 mM, pH = 4 and 25 °C).

4. Conclusions

This study examined the effects of dye concentration, pH, $Na_2S_2O_8$ dose and addition of $Na_2S_2O_8$, H_2O_2, Cu^{2+} and ethanol on a UV/TiO_2 system. Decolorization rate declined as dye concentration increased. The persulfate ions trapped photogenerated conduction band electrons, preventing the recombination of the electrons with positive holes and, simultaneously, generated sulfate free radicals. H_2O_2 trapped photogenerated electrons and inhibited the recombination of photogenerated electron/hole pairs. The k values for the UV/TiO_2, UV/TiO_2/$Na_2S_2O_8$ and UV/TiO_2/H_2O_2 systems increased with decreasing pH. Adding Cu^{2+} suppressed the recombination of photogenerated electron/hole pairs and generated additional persulfate free radicals in the UV/TiO_2/$Na_2S_2O_8$ system, thereby accelerating decolorization. The UV/TiO_2/H_2O_2/Cu system resembles the photo-Fenton-like process since the induced photo-Fenton-like reactions acted as an additional source of hydroxyl radicals. This investigation suggests that the primary decolorization pathway involves hydroxyl radicals and that direct oxidation by photogenerated holes is significant in the UV/TiO_2 system. During decolorization, some Cl^-, NO_3^- and SO_4^{2-} ions were released and, even when decolorization was complete, the TOC was reduced by only 50%.

Acknowledgements

The authors would like to thank the National Science Council of the Republic of China for financially supporting this research under Contract No. NSC 95-2221-E-212-022. Additionally, the partial experiments of this research by Ciao-Ying, Huang, Yu-Hsiang, Peng and Hui-Huang, Lin of Da-Yeh University were greatly appreciated.

References

[1] Konstantinou IK, Albanis TA. TiO_2-assisted photocatalytic degradation of azo dyes in aqueous solution: kinetic and mechanistic investigations − a review. Applied Catalysis B: Environmental 2004;49:1−14.

[2] Serpone N, Maruthamuthu P, Pichat P, Pelizzetti E, Hidaka H. Exploiting the interparticle electron transfer process in the photocatalysed oxidation of phenol, 2-chlorophenol and pentachlorophenol: chemical evidence for electron and hole transfer between coupled semiconductors. Journal of Photochemistry and Photobiology A: Chemistry 1995;85:247−55.

[3] Lo SC, Lin CF, Wu CH, Hsieh PH. Capability of coupled CdSe/TiO_2 for photocatalytic degradation of 4-chlorophenol. Journal of Hazardous Materials 2004;114:183−90.

[4] Wu CH. Comparison of azo dye decolorization efficiency using UV/single semiconductor and UV/coupled semiconductor systems. Chemosphere 2004;57:601−8.

[5] Wu CH, Chang CL. Decolorization of Procion Red MX-5B by advanced oxidation processes: comparative studies of the homogeneous and heterogeneous systems. Journal of Hazardous Materials 2006;128:265−72.

[6] Malato S, Blanco J, Richter C, Braun B, Maldonado MI. Enhancement of the rate of solar photocatalytic mineralization of organic pollutants by inorganic oxidizing species. Applied Catalysis B: Environmental 1998;17:347−56.

[7] Malato S, Blanco J, Maldonado MI, Fernandez-Ibanez P, Campos A. Optimising solar photocatalytic mineralization of pesticides by adding inorganic oxidizing species; application to the recycling of pesticide containers. Applied Catalysis B: Environmental 2000;28:163−74.

[8] Daneshvar N, Salari D, Khataee AR. Photocatalytic degradation of azo dye Acid Red 14 in water: investigation of the effect of operational parameters. Journal of Photochemistry and Photobiology A: Chemistry 2003;157:111−6.

[9] Daneshvar N, Salari D, Khataee AR. Photocatalytic degradation of azo dye Acid Red 14 in water on ZnO as an alternative catalyst to TiO_2. Journal of Photochemistry and Photobiology A: Chemistry 2004;162:317−22.

[10] Saquib M, Muneer M. TiO_2-mediated photocatalytic degradation of a triphenylmethane dye (Gentian Violet), in aqueous suspensions. Dyes and Pigments 2003;56:37−49.

[11] Qamar M, Saquib M, Muneer M. Photocatalytic degradation of two selected dye derivatives, Chromotrope 2B and Amido Black 10B, in aqueous suspensions of titanium dioxide. Dyes and Pigments 2005;65:1−9.

[12] Qamar M, Saquib M, Muneer M. Titanium dioxide mediated photocatalytic degradation of two selected azo dye derivatives, Chrysoidine R and Acid Red 29 (Chromotrope 2R) in aqueous suspensions. Desalination 2005;186:255−71.

[13] Tariq MA, Faisal M, Muneer M. Semiconductor-mediated photocatalysed degradation of two selected azo dye derivatives, Amaranth and Bismarck Brown in aqueous suspension. Journal of Hazardous Materials 2005;127:172−9.

[14] Bizani E, Fytianos K, Poulios I, Tsiridis V. Photocatalytic decolorization and degradation of dye solutions and wastewaters in the presence of titanium dioxide. Journal of Hazardous Materials 2006;136:85−94.

[15] Mohapatra P, Parida KM. Photocatalytic activity of sulfate modified titania 3: decolorization of methylene blue in aqueous solution. Journal of Molecular Catalysis A: Chemical 2006;258:118−23.

[16] Muruganandham M, Swaminathan M. Photocatalytic decolourisation and degradation of Reactive Orange 4 by TiO_2-UV process. Dyes and Pigments 2006;68:133−42.

[17] Faisal M, Tariq MA, Muneer M. Photocatalysed degradation of two selected dyes in UV-irradiated aqueous suspensions of titania. Dyes and Pigments 2007;72:233−9.

[18] Zhang T, Oyama T, Horikoshi S, Zhao J, Serpone N, Hidaka H. Photocatalytic decomposition of the sodium dodecylbenzene sulfonate surfactant in aqueous titania suspensions exposed to highly concentrated solar radiation and effects of additives. Applied Catalysis B: Environmental 2003;42:13−24.

[19] Liang C, Bruell CJ, Marley MC, Sperry KL. Persulfate oxidation for in situ remediation of TCE. II. Activated by chelated ferrous ion. Chemosphere 2004;55:1225−33.

[20] Carrier M, Perol N, Herrmann JM, Bordes C, Horikoshi S, Paisse JO, et al. Kinetics and reactional pathway of Imazapyr photocatalytic degradation. Influence of pH and metallic ions. Applied Catalysis B: Environmental 2006;65:11−20.

[21] Mahmoodi NM, Arami M, Limaee NY. Photocatalytic degradation of triazinic ring-containing azo dye (Reactive Red 198) by using immobilized TiO_2 photoreactor: bench scale study. Journal of Hazardous Materials 2006;133:113−8.

[22] Shimizu N, Ogino C, Dadjour MF, Murata T. Sonocatalytic degradation of methylene blue with TiO_2 pellets in water. Ultrasonics Sonochemistry 2007;14:184−90.

[23] Dogliotti L, Hayon E. Flash photolysis of persulfate ions in aqueous solutions. Study of the sulfate and ozonide radical anions. The Journal of Physical Chemistry 1967;71:2511−6.

[24] Ivanov KL, Glebov EM, Plyusnin VF, Ivanov YV, Grivin VP, Bazhin NM. Laser flash photolysis of sodium persulfate in aqueous solution with addition of dimethylformamide. Journal of Photochemistry and Photobiology A: Chemistry 2000;133:99−104.

[25] Wang KH, Hsieh YH, Wu CH, Chang CY. The pH and anion effects on the heterogeneous photocatalytic degradation of *o*-methylbenzoic acid in TiO_2 aqueous suspension. Chemosphere 2000;40:389−94.

[26] House DA. Kinetics and mechanism of oxidations by peroxydisulfate. Chemical Reviews 1962;62:185−203.

[27] Kusic H, Koprivanac N, Bozic AL, Selanec I. Photo-assisted Fenton type processes for the degradation of phenol: a kinetic study. Journal of Hazardous Materials 2006;136:632−44.

[28] Modirshahla N, Behnajady MA, Ghanbary F. Decolorization and mineralization of C.I. Acid Yellow 23 by Fenton and photo-Fenton processes. Dyes and Pigments 2007;73:305−10.

[29] Buxton GV, Greenstock CL, Helman WP, Ross AB. Critical review of rate constants for reactions of hydrated electrons, hydrogen atoms and hydroxyl radicals ($OH^{\bullet}/O^{-\bullet}$) in aqueous solution. Journal of Physical and Chemical Reference Data 1988;17:513−886.

[30] Wardman P. Reduction potential of one-electron couples involving free radicals in aqueous solution. Journal of Physical and Chemical Reference Data 1989;18:1637−755.

[31] Skoumal M, Cabot PL, Centellas F, Arias C, Rodriguez RM, Garrido JA, et al. Mineralization of paracetamol by ozonation catalyzed with Fe^{2+}, Cu^{2+}, and UVA light. Applied Catalysis B: Environmental 2006;66:228−40.

[32] Litter MI. Heterogeneous photocatalysis: transition metal ions in photocatalytic systems. Applied Catalysis B: Environmental 1999;23:89−114.

[33] Lam SW, Chiang K, Lim TM, Amal R, Low GK-C. Effect of charge trapping species of cupric ions on the photocatalytic oxidation of resorcinol. Applied Catalysis B: Environmental 2005;55:123−32.

[34] Wawrzyniak B, Morawski W. Solar-light induced photocatalytic decomposition of two azo dyes on new TiO_2 photocatalyst containing nitrogen. Applied Catalysis B: Environmental 2006;62:150−8.

[35] Silverstein RMC, Basdler GC, Morrill GC. Spectrophotometric identification of organic compounds. New York: Wiley; 1991.